

DYNAMIC CRACK RESISTANCE OF ACRYLIC PLASTIC

V. P. Efimov and E. N. Sher

UDC 539.375

The dependence of the stress-intensity factor near the tip of a growing crack in an SO-120 acrylic plastic on the crack-propagation velocity $K_I(v)$ within the range of 10^{-5} –300 m/sec is determined. Specific features of crack propagation associated with the shape of the curve $K_I(v)$, which has discontinuities and nonuniqueness intervals, are discussed.

Brittle failure of solids due to growing cracks occurs in many mining processes, for example, in contour explosion, explosive crushing of rocks, hydraulic fracturing, and mechanical failure. It also has a considerable effect on the lifetime of constructions and buildings. In engineering practice, the crack resistance of a material to brittle failure is characterized by the critical stress-intensity factor for plane strain K_{Ic} . A crack begins to grow when the stress-intensity factor K_I exceeds the critical value: $K_I > K_{Ic}$. The parameter K_{Ic} is determined by the moment the crack starts to grow. Within the framework of the linear fracture mechanics, the dependence of the stress-intensity factor on the crack rate $K_I(v)$ (dynamic curve of crack resistance) fully characterizes the crack resistance of a given material at constant temperature and humidity.

Experimental determination of the entire dynamic curve $K_I(v)$ involves many difficulties, and therefore, a simplified analysis is commonly used, in which the minimum value K_{Im} of the curve $K_I(v)$ is taken to be the criterion of termination or growth of the crack. For $K_I < K_{Im}$, the crack does not propagate. The value of K_{Im} can differ from K_{Ic} . An analysis of dynamic cracks in the start–stop regime [1] shows that, for some materials, the value of K_{Im} is equal to the stress-intensity factor at the moment the crack stops K_{Ia} , and it is smaller than K_{Ic} . Using this criterion, one can predict where the crack stops under given conditions. However, the crack propagation with time and, hence, the failure parameters or service life of a construction cannot be calculated without knowledge of the entire curve $K_I(v)$. Consequently, it is of practical importance to determine the entire dynamic crack-resistance curve for various rocks and structural materials. At present, the studies are performed by optical methods for a number of transparent materials which are also used to model brittle failure. The acrylic plastic polymethylmethacrylate (PMMA) is a model material. Its crack resistance was studied in [2–6]. Slow cracks were considered in [2–5] within the velocity range from 10^{-7} to 10^{-2} m/sec. Green and Pratt [6] gave data on crack resistance for crack-propagation velocities within the range from 100 to 600 m/sec and supplemented these data by the values of crack resistance of slow cracks borrowed from [4, 5]. The resulting crack-resistance curve should be refined, since it is not clear whether the same material was used in the tests [6] on slow and fast cracks. PMMA is a wide class of one-type plastics different in composition and mechanical properties. This fact was ignored in [6]. The resulting crack-resistance curve of PMMA is fairly complex. It is not monotonic and has discontinuities. There is a velocity range in the curve for which no data on the existence of propagating cracks are available. Indeed, according to data published within the literature, no propagation of cracks was observed in PMMA specimens in the velocity range from 10 cm/sec to 80 m/sec.

The aim of this paper is to determine the entire crack-resistance curve for one material (industrial acrylic plastic SO-120 from the PMMA class) and to refine the specific features of crack propagation within the above-mentioned range of their velocities.

Mining Institute, Siberian Division, Russian Academy of Sciences, Novosibirsk 630091. Translated from *Prikladnaya Mekhanika i Tekhnicheskaya Fizika*, Vol. 42, No. 5, pp. 217–225, September–October, 2001. Original article submitted December 8, 2000; revision submitted February 26, 2001.

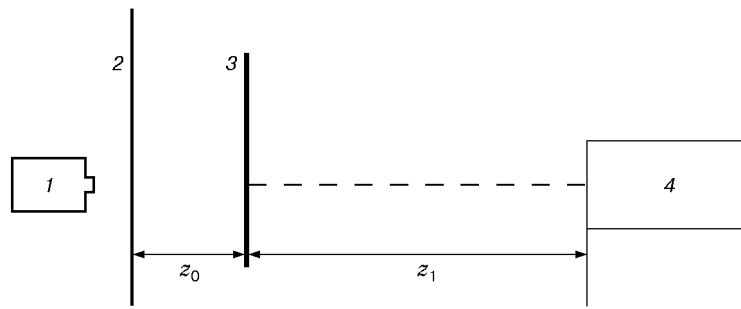


Fig. 1. Experimental scheme: 1) camera; 2) screen; 3) specimen; 4) light source [(He-Ne)-laser or spark stroboscope].

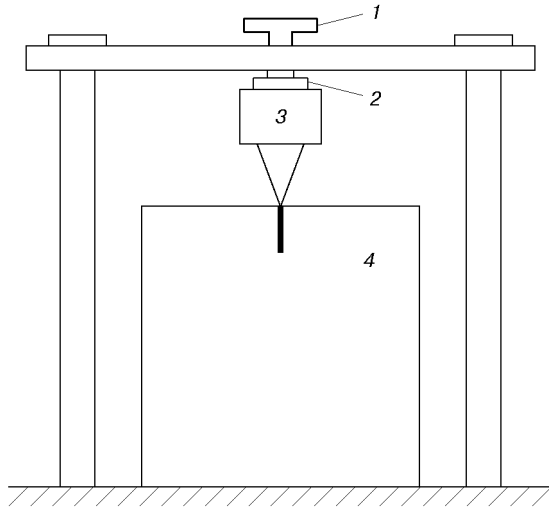


Fig. 2

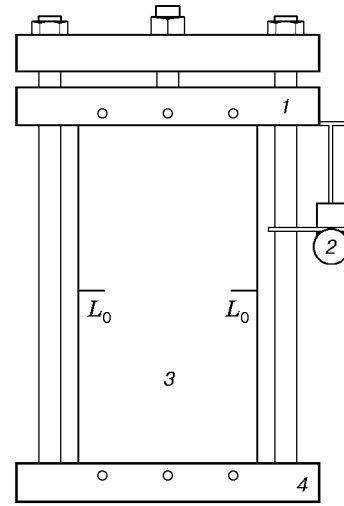


Fig. 3

Fig. 2. Loading scheme: 1) loading screw; 2) elastic element; 3) wedge; 4) specimen.

Fig. 3. Scheme of extension of a specimen with edge cuts: 1) movable grip; 2) displacement indicator; 3) specimen; 4) immovable grip.

Measurement of Crack Resistance. The stress-intensity factors were determined by the shadow method [7] with the use of the formula

$$K_I = \frac{2\sqrt{2\pi}}{3z_0 t_0 c} \frac{1}{\lambda^{3/2}} \left(\frac{D}{\delta} \right)^{5/2},$$

where D is the diameter of a caustic registered on the screen, z_0 is the distance from the object to the screen, t_0 is the thickness of the specimen, c is the material constant determined by the optical and mechanical properties, λ is the magnification of the optical scheme of the experiment determined by the properties of the light source and the distances z_0 and z_1 (Fig. 1), and δ is a numerical coefficient. To record the shadow figures, we used a photographic camera and a spark stroboscope with controllable relative pulse duration or a video camera. This recording scheme (Fig. 1) allowed us to determine the position of the crack and the stress-intensity factor for cracks propagating with a velocity up to 200 m/sec. Efimov [8] determined the crack resistance of an SO-120 acrylic plastic for velocities of 100 m/sec and higher. Slow cracks in a continuously illuminated specimen were recorded by a video camera. The crack velocities recorded distinctly by an ordinary video camera lie within the range from 10^{-4} to 1 m/sec. Thus, this photography method allowed us to record propagating cracks in the entire velocity range of interest. The error in measuring the stress-intensity factors by the shadow method was 5%.

The loading scheme and the shape of specimens were chosen to ensure smooth variation in the stress-intensity factor on a large segment of the crack trajectory. To record the crack resistance by the crack-arrest method, it is

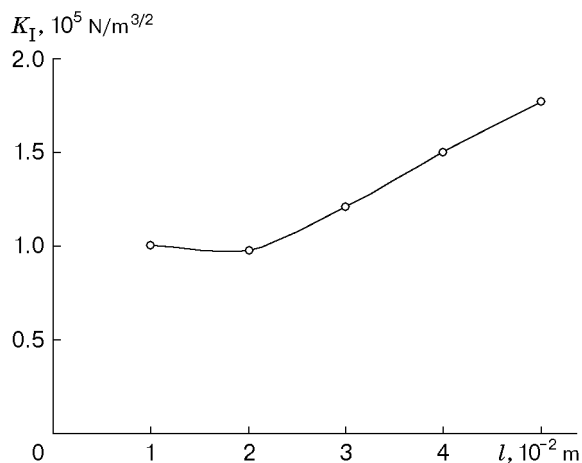


Fig. 4

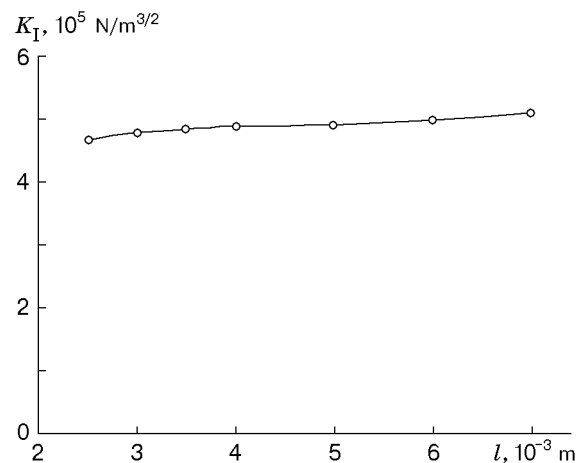


Fig. 5

Fig. 4. Stress-intensity factor K_I versus the crack length l for a 10×10 cm compact specimen loaded by a 45° wedge with a force of 10^4 N/m.

Fig. 5. Predicted stress-intensity factor K_I for a specimen with two edge cuts versus the length of one of the cuts (the size of the specimen is 10×20 cm, the initial length of the cuts is $l_0 = 2.5$ cm, and the elongation is 0.2 mm).

desirable to have a monotonically decreasing dependence $K_I(l)$. To study the transition from a slow to a fast crack, a smoothly increasing branch of the curve $K_I(l)$ is necessary. An important condition of experimental repetition is the stability of the crack trajectory. In testing specimens of the same type, it was impossible to satisfy all the above-mentioned requirements; therefore, the following two loading cases were considered: wedging out a compact cracked specimen (scheme No. 1 in Fig. 2) and extension of a specimen with two edge cuts (scheme No. 2 in Fig. 3). Figure 4 shows the stress-intensity factor versus the crack length $K_I(l)$ for a square specimen loaded by a 45° wedge with a force of 10^4 N/m for a coefficient of friction of the wedge over acrylic plastic $\mu = 0.12$ [9]. The curve has a linearly increasing segment in the middle part of the specimen. Varying the stiffness of the elastic element in these tests, we obtained different velocity regimes of crack propagation: from accelerating regimes at constant force to decelerating regimes for stiff loading. Specimens were wedged out at a constant penetration velocity of the wedge with the use of an UMÉ-10T test machine. In this case, the condition of smooth variation in $K_I(l)$ was not satisfied, and the crack propagated discontinuously. The wide range of the feed rate of the cross-piece of the test machine made it possible to extend the velocity range of slow cracks. To study the transition from slow to fast failure in more detail, we used scheme No. 2. Figure 5 shows the predicted stress-intensity factor $K_I(l)$ at the tip of a growing crack for the case where the second crack is immovable and the elongation of the specimen is constant.

Experimental Technique. According to scheme No. 1, $100 \times 100 \times 10$ mm specimens were loaded by 30 and 45° steel wedges. Slow cracks propagating with a velocity of less than 1 cm/sec were studied under static loading of the specimens (see Fig. 2). The use of an elastic vacuum-rubber element 30 mm in diameter and 5–10 mm thick allowed us to obtain a weakly decreasing dependence of the stress-intensity factor $K_I(l)$ in the middle part of the specimen. The specimen had a cut along the centerline with a sharp tip or a crack at its end, which enabled us to vary the initial velocity regime of the crack. Fast cracks were obtained by loading the specimen by the same wedges using an UMÉ-10T test machine. To study the deceleration and termination regimes of the cracks whose velocity was less than 100 m/sec, the specimen was loaded by a wedge falling from a small height to avoid complete splitting of the specimen.

To study the transition from slow to fast propagation of the crack for a constant stress-intensity factor K_I , the specimens were loaded with the use of a breakage device for constant elongation according to scheme No. 2. Two symmetric cuts were made in a plane $120 \times 240 \times 4$ mm specimen fixed in the grips of the device. An initial crack was made on the continuation of one of the cuts. The length of the cuts with allowance for the initial crack was identical for each specimen and varied from one specimen to another within 24–30 mm. To measure the velocity of the cracks, thin copper wires 0.02 mm in diameter were glued to the specimen by cyanoacrylate adhesive transversely to the direction of propagation of the cracks. The wires were 2 mm apart, and the distance from the tip of the

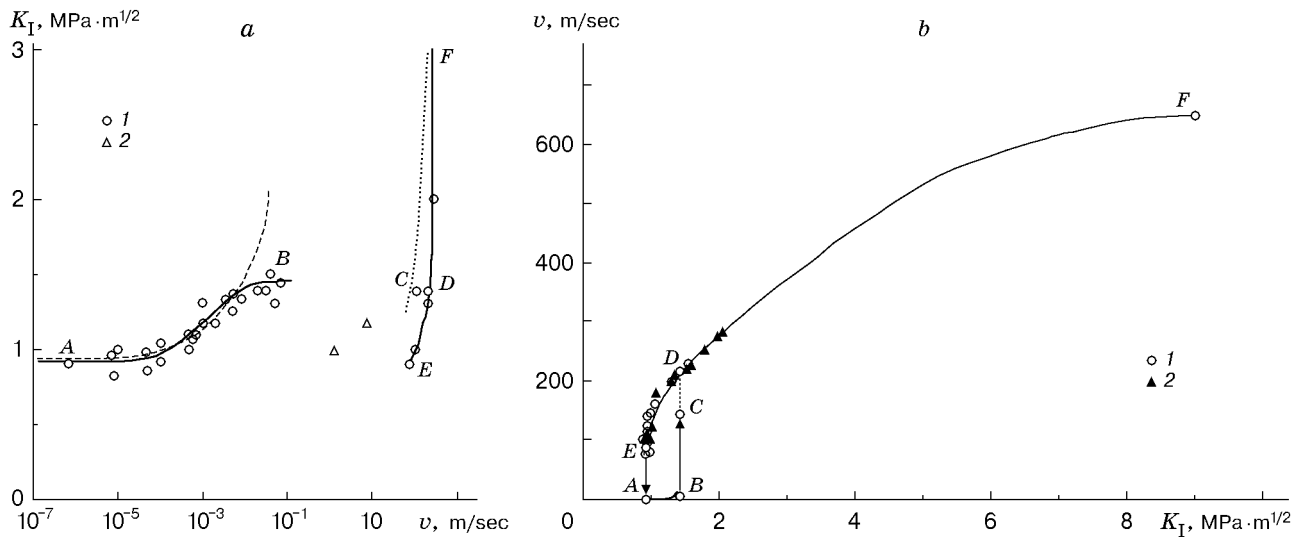


Fig. 6. Stress-intensity factor versus the velocity of a crack for a PMMA specimen (points are the experimental data and curves are the averaged data): (a) the solid curves and points 1 refer to the results of the present study, the dashed curve and points 2 refer to the data of [4, 5], and the dotted curve shows the data of [6]; (b) points 1 refer to accelerating cracks and points 2 refer to decelerating cracks; the solid curve shows the data of [6].

initial crack to the nearest wire was 2 mm. Failure of the wires was determined with the use of an S8-9 oscillograph. Elongation of the specimen was measured by a clock-type indicator with an error of 0.005 mm.

Experiments and Results. In tests performed in accordance with scheme No. 1 (see Fig. 2), a square specimen was loaded by a wedge by turning the loading screw through the elastic element. The shadow pattern of failure from the crack starting to the failure of the specimen was recorded on the projection screen by a video camera. Before tests, a nucleation crack was initiated on the continuation of a cut, from which the main crack started. For a nucleus shaped like an ideal plane cut, the crack began to propagate at low stress and ran gradually across the entire specimen. In specimens with a sharp cut and without nuclei, the initial velocity of the crack increased. In this case, the crack propagated through the specimen with a considerable variation in velocity, but video recording allowed us to determine characteristic regions in the specimen where the crack propagation was quasi-stationary. The fractography analysis of the fragments clearly shows these regions characterized by different velocity regimes. Thus, each test specimen gave one or more points on the dynamic crack-resistance curve.

Figure 6a shows the experimentally determined stress-intensity factor versus the propagation velocity of the crack. The use of the loading device (see Fig. 2) allowed us to study cracks propagating with a velocity lower than 1 cm/sec. Experiments performed on an UMÉ-10T test machine were very similar to those described above, but in this case, the velocity range that could be studied by a video camera was extended to 5 cm/sec. In using the test machine, cracks propagated, as a rule, by jumps, only some of which could be determined in the subsequent analysis. If crack propagation were uniform within the period of a frame, the velocity observed in the experiment would be as high as 0.8 m/sec. However, there were frames in which two positions of the crack were seen. A comparison of the video record and the results of the fractography analysis shows that the first position of the crack corresponds to its start and the second position to its stop. This suggests that, upon attaining a certain limiting velocity, the crack performs jumps characterized by a high velocity, and the recorded positions of the crack correspond to its stop for a short time. In some cases, these stops are recorded in one frame, but more often in two neighboring frames. The caustics recorded in this case have a distinct structure. The diameter of the caustics before a jump is 10–15% larger than that at the moment of stop, the difference between the stress-intensity factors being approximately 30–40%. For SO-120, the stationary velocity before a jump determined by means of the video camera was 5 cm/sec and the corresponding stress-intensity factor was $1.4 \text{ MPa} \cdot \text{m}^{1/2} \pm 10\%$. Video recording did not allow us to determine the transient regimes where the stationary slow propagation of a crack becomes fast and, vice versa, where the fast propagation of a crack is followed by its stop.

To clarify the character of discontinuous propagation of a crack and to study the transient regimes, we performed recording with the use of a spark stroboscope. Caustics were photographed by superimposing one frame

onto another. The calibration of a new illumination scheme and recording of the caustics were performed for a slow crack propagating with a velocity of the order of 1 mm/sec. A thin wire was glued to the specimen, and its failure generated a synchronizing pulse to initiate the stroboscope. The specimen was loaded by a wedge falling from a small height such that the crack stopped after it passed 1–3 cm. In these experiments, we failed to refine the velocity of transition from slow to fast propagation of the crack, but we obtained data on decelerating cracks whose minimum velocity was 75 m/sec. The stress-intensity factor for cracks propagating at 75 m/sec had the least value equal to $0.9 \text{ MPa} \cdot \text{m}^{1/2}$. The error in measuring the stress-intensity factors was 5% and the statistical scattering was 10%. In many experiments, temporal stops of the cracks were observed. The stress-intensity factor K_{Ia} for cracks that ceased to propagate was $0.9 \text{ MPa} \cdot \text{m}^{1/2}$ as in the case where the velocity was 75 m/sec. For both static and dynamic loading of the specimens by a wedge, we failed to study the propagation of decelerating cracks at velocities lower than 75 m/sec.

We attempted to refine the data on the velocity of cracks in specimens covered by a wire net that allowed us to determine the position of the crack with a step of 2 mm. Using this technique, we could calculate only the average velocity between the wires. In the intervals between the wires where the crack ceased to propagate, the velocity was low, but these intervals were determined well by the fractography analysis. The values of the velocities obtained were ignored. A similar pattern of correlation of intervals characterized by low velocity with marks corresponding to stop of the crack was observed in [10]. The results of these experiments confirm the conclusion that the minimum velocity is 75 m/sec. In experiments where high-speed photography was performed by an SFR-1 photochronograph [11], no propagation of cracks in the deceleration regime at velocities lower than 75 m/sec was observed either, though the geometry of specimens and the scheme of loading were different in this case. Thus, for a constant value of K_I equal to the minimum value, the crack propagated with stops. During propagation, its velocity was 75 m/sec.

The transient regime where a slow crack became fast was studied with the use of specimens extended by a rigid breakage device (scheme No. 2). For this way of loading, the stress-intensity factor for a propagating crack remained almost unchanged, and therefore, the crack propagated with low velocity almost through the entire specimen. The transient regime was caused by a small strain of the specimen after the beginning of propagation. In this case, initially, the crack propagated slowly with a small acceleration in the interval about 1 cm, and then it abruptly entered the dynamic regime with a velocity exceeding 100 m/sec. In studying these phenomena, the main difficulty is that the entire process cannot be recorded by an oscillograph. A wide range of velocities from 10^{-2} m/sec at the initial stage to 10^2 m/sec for dynamic propagation and the time spread of transition from one region to another lead to the fact that, for a low sweep speed of the oscillograph for a fixed initial stage, one cannot perform measurements if the crack propagates quickly. To avoid this situation, we used two oscillographs, one of which was initiated from the first wire of the net sensor with long sweep and the other was initiated from the last wire in the prerecording regime. The sweep of the second oscillograph was chosen so as to record the dynamic regime of the crack propagation reliably.

After a number of tests in accordance with scheme No. 2, we succeeded in considering the transient regime in more detail. For the chosen geometry, the crack is gradually accelerated up to a velocity of 20 cm/sec, and then it enters abruptly the dynamic regime with an initial velocity of 140 m/sec. Its further behavior depends on the loading conditions.

Using the experimental results, we plotted the dynamic curve of crack resistance of SO-120 with the use of the logarithmic (Fig. 6a) and linear (Fig. 6b) scales for velocity. The curve consists of three branches: the branch *AB* corresponds to slowly propagating cracks, the branch *BCD* to accelerating cracks only, and the branch *EDF* to accelerating and decelerating cracks. There are some characteristic points on the curve: at the point *A*, the stress-intensity factor reaches the minimum value $K_I = 0.9 \text{ MPa} \cdot \text{m}^{1/2}$, which corresponds to starting of slow cracks; at the point *B*, the velocity of slow propagation of the crack is maximum ($v = 0.2 \text{ m/sec}$ and $K_I = 1.4 \text{ MPa} \cdot \text{m}^{1/2}$); at the point *C*, the crack begins to propagate quickly ($v = 140 \text{ m/sec}$ and $K_I = 1.4 \text{ MPa} \cdot \text{m}^{1/2}$); at the point *E*, the velocity and the stress-intensity factor immediately before the crack stops are $v = 75 \text{ m/sec}$ and $K_I = 0.9 \text{ MPa} \cdot \text{m}^{1/2}$; at the point *D* ($v = 200 \text{ m/sec}$ and $K_I = 1.4 \text{ MPa} \cdot \text{m}^{1/2}$), the branches *BCD* and *EDF* merge together.

Figure 6 shows also the curves of crack resistance of PMMA given in [4–6]. They differ from the curves obtained in the present work in that, according to our results, the stress-intensity factor immediately before the crack stops K_{Ia} (point *E*) is minimum not only for the dynamic branch of the curve but also for the entire crack-resistance curve, i.e., the minimum dynamic stress-intensity factor is very close to the crack resistance of very slow cracks. In the velocity range from 0.2 to 75 m/sec, no cracks were observed in the present study. It is likely that the data on crack velocities given in [4, 5] are averaged and determined without allowance for instant stops. An

insignificant quantitative discrepancy between the data of [4–6] and the values of crack resistance obtained in the present work can be attributed to the fact that each curve was determined for different materials from the PMMA class.

Discussion of Results. The crack-resistance curve obtained shows that the propagation of a crack has some specific features. In propagation intervals where $dK_I/dl > 0$, the velocity of the crack increases continuously. The failure of a strip with an edge crack under increasing stress is an example where this condition holds. Under these conditions, the crack is unstable and, after starting, it is accelerated and splits the specimen. As an example, we consider the failure of a 120×240 mm specimen from an SO-120 acrylic plastic with an initial edge crack 28 mm long. The failure proceeds as follows: the crack starts to grow slowly for $K_I = 0.93 \text{ MPa} \cdot \text{m}^{1/2}$; then, it is accelerated, grows up to 43 mm, and enters the fast-propagation regime. At the moment of the instability of the crack (transition to the fast-propagation regime), the stress-intensity factor is $K_I = 1.5 \text{ MPa} \cdot \text{m}^{1/2}$. The time of slow propagation of the crack is 15 sec. In the phase plane in the coordinates (K_I, v) , the propagation of the crack is described as follows: the phase point corresponding to the propagating crack moves along the crack-resistance curve from the point *A* to the point *B* (Fig. 6a). Then, the crack enters the dynamic regime, and its velocity abruptly increases up to a value corresponding to the point *C*. Afterward, the crack is accelerated, and its phase point passes to the branch *DF* on the crack-resistance curve (Fig. 6b).

If the loading conditions are such that $dK_I/dl < 0$ for a certain segment of the trajectory of the crack, it is decelerated. The corresponding phase point moves to the left along the branch *FE* (Fig. 6b) and reaches the point *E*, at which the crack stops. Our observations show that, if K_I decreases after the crack stops and then increases, new growth of the crack is possible. For an SO-120 acrylic plastic, we found that, if the time during which the crack rests is short (less than $5 \mu\text{sec}$), the propagation is recommenced at velocities corresponding to the branch *ED* of the crack-resistance curve. Figure 6b shows the experimental values of the crack resistance of accelerating and decelerating cracks. One can see that the branch *EF* corresponds to both accelerating and decelerating cracks, whereas the branch *BD* to accelerating cracks only. It follows that, at the initial stage of failure, the point corresponding to crack propagation is bound to pass along the branches *AB* and *BD* before entering the branch *EDF*. The same behavior of cracks was described in [12, 13] for some epoxy polymers.

The experimental dependence of crack resistance of a material on the crack velocity is used to calculate the dynamics of brittle fracture. Sher [14] proposed the relation $K_I(v)$ for acrylic plastic in the form

$$v = V_0[1 - \exp(1 - K_I/K_{Ic})], \quad (1)$$

where $V_0 = 650 \text{ m/sec}$ and $K_{Ic} = 1.2 \text{ MPa} \cdot \text{m}^{1/2}$. This relation satisfactorily describes the failure of a brittle medium subjected to an explosion or impact. In this case, the crack growth at the stage of slow propagation is reasonably small. To construct the curve $K_I(v)$, one should take the refined value of the stress-intensity factor corresponding to the stop $K_{Ia} = 0.9 \text{ MPa} \cdot \text{m}^{1/2}$ (point *E* in Fig. 6a) rather than the value $1.2 \text{ MPa} \cdot \text{m}^{1/2}$ determined from (1). As a whole, the curve $K_I(v)$ (Fig. 6b) can be approximated analytically by the piecewise smooth function

$$\begin{aligned} v &= V_0 \exp \alpha(K/K_0 - 1) & \text{for } 0 < v < 0.2 \text{ m/sec (branch AB),} \\ v &= V_1[1 - \exp \beta(1 - K/K_D)] & \text{for } v > 75 \text{ m/sec (branch EF).} \end{aligned} \quad (2)$$

Here $V_0 = 10^{-5} \text{ m/sec}$, $K_0 = 1.4 \text{ MPa} \cdot \text{m}^{1/2}$, $K_D = 0.6785 \text{ MPa} \cdot \text{m}^{1/2}$, $\alpha = 16.57$, $V_1 = 670 \text{ m/sec}$, and $\beta = 0.268$.

In calculations by formulas (2), it is necessary to take into account the history of crack propagation and the sign of its acceleration.

Approximation (2) was used to estimate the crack length L_1 before its rapid growth in a specimen with an edge crack in the above-considered example. The calculated value is $L_1 = 43 \text{ mm}$, which is close to the experimental value.

Conclusions. The results obtained can be summed up as follows.

The curve $K_I(v)$ for PMMA has three branches: the branch of slow cracks, the branch of accelerating fast cracks only, and the branch of accelerating and decelerating fast cracks.

Specific features of propagation of a crack upon its acceleration and deceleration have been determined. At the initial stage of failure, the crack grows slowly and then abruptly enters the acceleration branch with higher values of K_I .

An analytical approximation of the experimental curve $K_I(v)$ has been proposed.

This work was supported by the Russian Foundation for Fundamental Research (Grant No. 01-0100829).

REFERENCES

1. P. Crosley and E. Ripling, "Specific features of crack propagation in the start-stop interval," in: *Fracture Mechanics. Fast Failure and Stop of Cracks* [Russian translation], Vol. 25, Mir, Moscow (1981), pp. 74–100.
2. A. S. Vavakin and R. L. Salganik, "Crack resistance of acrylic plastic," *Izv. Akad. Nauk SSSR, Mekh. Tverd. Tela*, No. 4, 167–175 (1971).
3. V. I. Aleshin, É. L. Aero, E. B. Kuvshinskii, and I. A. Slavitskii, "Kinetics of crack growth in acrylic plastic plates," *Izv. Akad. Nauk SSSR, Mekh. Tverd. Tela*, No. 2, 70–79 (1981).
4. J. G. Williams, J. C. Radon, and C. E. Turner, "Designing against fracture in brittle plastics," *J. Polymer Eng. Sci.*, **8**, No. 2, 130–139 (1968).
5. J. G. Williams, "Visco-elastic and thermal effects on crack growth in PMMA," *Int. J. Fracture Mech.*, **8**, 393–398 (1972).
6. A. K. Green and P. L. Pratt, "Measurement of the dynamic fracture toughness of the polymethylmethacrylate by high speed photography," *Eng. Fracture Mech.*, **6**, No. 1, 71–80 (1974).
7. P. S. Teokaris, "Local flow near a crack tip in acrylic plastic," *Prikl. Mekh.*, No. 2, 159–165 (1970).
8. V. P. Efimov, "Dynamic calibration of measuring the crack resistance of brittle materials by wedge loading," *Fiz. Tekh. Probl. Razrab. Polez. Iskop.*, No. 4, 89–93 (1990).
9. V. P. Efimov, P. A. Martynyuk, and E. N. Sher, "Taking into account the vertical forces in wedge tests," *Fiz. Tekh. Probl. Razrab. Polez. Iskop.*, No. 3, 32–36 (1992).
10. J. Kolgton and B. Denton, "Measurement of fast crack growth in metals and nonmetals," in: *Fracture Mechanics. Fast Failure and Stop of Cracks* [Russian translation], Vol. 25, Mir, Moscow (1981), pp. 174–198.
11. E. N. Sher, "Study of the dynamics of crack propagation by the photoelastic method," *Prikl. Mekh. Tekh. Fiz.*, No. 6, 150–158 (1974).
12. T. Koboyashi and J. Dally, "Relation between the velocity of a crack and the stress-intensity factor in polymers with double refraction," in: *Fracture Mechanics. Fast Failure and Stop of Cracks*, Vol. 25 [Russian translation], Vol. 25, Mir, Moscow (1981), pp. 101–119.
13. N. I. Kashevarova and E. N. Sher, "Experimental study of crack deceleration in an optically active epoxy material," *Izv. Akad. Nauk SSSR, Mekh. Tverd. Tela*, No. 3, 182–185 (1983).
14. E. N. Sher, "Calculation of propagation of radial cracks formed upon an explosion in a brittle medium in a quasistatic approximation," *Fiz. Tekh. Probl. Razrab. Polez. Iskop.*, No. 2, 40–42 (1982).